About 10 to 12 percent of the passenger automobiles in the area had studded rear tires. These tires seem to be the main cause of reflector wear, and where they are allowed, the use of shields on reflectors is advantageous. Under conditions in which the lifetime of reflectors is short, the ease of replacement when spring clamps are used and the consequent lower labor costs may balance the higher reflector loss of this type of assembly. Further study of large-scale installations of the marker over a period of 3 or more years in several areas with a wide range of snowfall rates and uses of studded tires should provide useful information for predicting annual losses. The relation between the amount of reflector surface damaged and the nighttime visibility of the reflector should be investigated. This information could be used to determine when replacement is warranted.

ACKNOWLEDGMENTS

We wish to acknowledge the assistance given by E. F. Reilly, R. L. Hollinger, J. J. Gertler, and Richard Weed of the Division of Research and Development and the Bureau of Maintenance, New Jersey State Department of Transportation. The technical assistance provided by Larry Smith, Robert Flanagan, and Adam Smorzaniuk of the Amerace Corporation and the funding and active support of the Materials Division of the Office of Research, Federal Highway Administration, is also appreciated.

Publication of this paper sponsored by Committee on Mineral Aggregates.

Test for the Adhesion of Thermoplastic Highway-Marking Materials

James S. Noel and Steven D. Hofener, Texas Transportation Institute, Texas A&M University

A new method for evaluating the adhesion between thermoplastic highway-marking materials and pavement surfaces is described. The specimen consists of a small square block of paving material (e.g., Portland cement concrete, asphaltic concrete, or some other) with a layer of thermoplastic bonded to one surface. An orifice penetrates the block and opens into a small circular area intentionally not bonded. A blister is formed by forcing fluid through the orifice until the diameter of the unbonded area begins to grow. The pressure used to inflate the blister and the height at the center of the blister are simultaneously recorded. From these measured data, the characteristic adhesive strain energy release rate is calculated. The analytical expressions necessary for the calculations are given, as is a discussion of the significance of the results to the highway engineer. Several exploratory tests were performed and the results are reported. The results demonstrate the sensitivity of the test to the adhesion of the thermoplastic to the pavement surface. Thus, the test can be used to quantify the effect on adhesive strength of those field conditions that can be reproduced in the laboratory.

Thermoplastic highway-marking materials have several advantages over conventional paints. These include better durability, improved color retention, and greater nighttime visibility, especially during periods of heavy rainfall. However, they also have disadvantages: (a) a tendency to flake during the winter (1) and (b) a tendency to blister shortly after placement, especially in the southern states. Figure 1 shows both phenomena and the accelerated degradation that results under the action of traffic.

Both of these disadvantages are related to the degree of adhesion between the marking material and the pavement. This adhesive strength varies, depending on the type of pavement, the time of cure, and the environment. The type of pavement is extremely important; the thermoplastics are much more durable on asphalt than on portland cement concrete. On either, the durability can be improved by the application of a chemical bonding agent before placing the thermoplastic.

Many makeshift methods of testing adhesion to pavements have evolved; however, the results are qualitative and can be only used for comparative purposes. Thus, the selection and method of applying these thermoplastics and primers has generally been left to the judgment of the responsible engineer. This judgment is typically developed through field experience and performance testing—a long, costly process.

A laboratory test toward the same end is suggested here. The test is based on the validity of the energy approach to adhesive fracture. A similar test was originally proposed for use with conventional paint in 1961 by Dannenberg (2). The approach has recently been developed and discussed in detail in a series of papers by Williams and his coworkers (3, 4, 5, 6). These studies concluded that there exists a system parameter (γ), the characteristic adhesive fracture energy, that quantitatively reflects the resistance of a bonded surface to the growth of an unbonded area. This parameter may be sensitive to the rate of loading and the temperature, but is independent of geometry. If the stiffnesses of the adherends and the γ are known, a stress analysis of any geometry can be used to establish the critical balance between the change in the potential energy of the system and γ. The following discussion of the analytical expressions for the energy balance of the blister-test geometry is based on the references cited above.

ANALYTICAL APPROACH

Consider an axially symmetric structure consisting of a flat infinite surface covered by a layer of a second material. The covering layer is bonded to the surface, except for a circular area centered about an axis of symmetry. An orifice smaller in diameter than the unbonded area penetrates the substrate (Figure 2a).

To perform the test, a fluid is forced through the orifice, causing the unbonded portion of the covering plate to deform upward, i.e., blister. The fluid used can be either compressible or incompressible. If it is

Figure 1. Thermoplastic stripe on a grooved pavement surface after two winters of service.

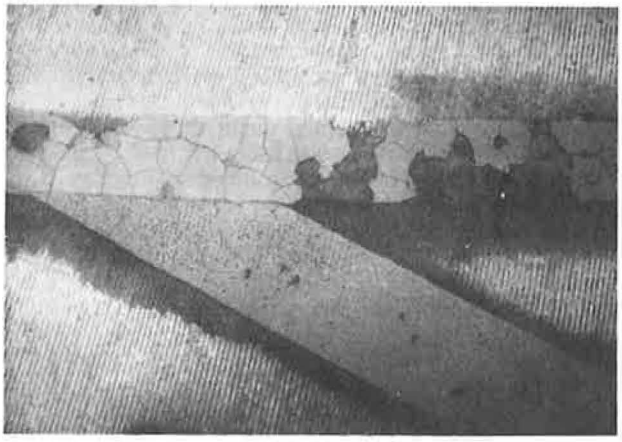

Figure 2. Phases of bond test: (a) initially unbonded area, (b) blister formed, and (c) blister extended.

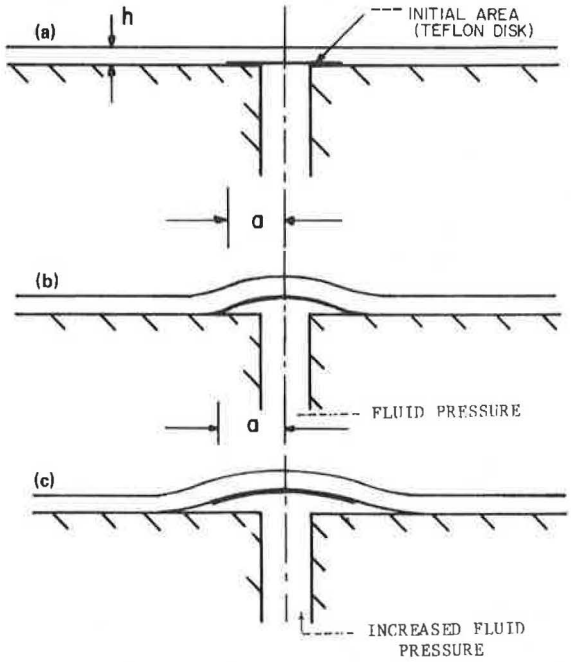

compressible, the analytical interpretation must use traction (pressure) boundary conditions applied to the underside of the blister; if it is incompressible, the analytical expression must use displacement (volume) boundary conditions. The difference between the two is quite important, in a philosophical sense and in the required laboratory technique. But, as shown in the derivations below, the algebraic expressions for criticality are ultimately identical.

The rather simple derivations for fracture in a homogeneous body begin with a functional representative of the potential energy (PE) of the system, including a term for the free surface energy, that can be written as

$$PE = \int_V U dv - \int_S T_i u_i ds - \int_S \gamma ds \qquad (1)$$

where the first term represents the strain energy density (U), integrated over the total volume of the body (V), the second term represents the tractions in the ith direction (T_i) multiplied by the corresponding displacements (u_i), integrated over the free surface area (S), and the last term represents the energy of γ, also integrated over S. This expression is of little physical consequence except that it always assumes a minimum value when the body is displaced into an equilibrium state. Thus, for equilibrium

$$\delta PE = 0 \qquad (2)$$

where the variation is not only of u, but also of a crack shape and size. Accordingly, the theorem of minimum potential energy (7, p. 385) can be rephrased as

> Of all the displacements, and crack configurations, satisfying the given boundary conditions, those which satisfy the equilibrium equations make the potential energy an absolute minimum.

Consequently, an expression for crack-growth criticality can be derived by evaluating the terms of Equation 1, assuming a crack-growth geometry, and taking the derivative with respect to a characteristic crack dimension. The value of zero for this derivative will define the configuration corresponding to the minimum potential energy and, in turn, the equilibrium.. If, at a given crack size, the derivative of the potential energy is decreasing, the crack will grow; otherwise it will not.

EXPRESSIONS FOR CRITICALITY

Consider a blister being inflated (Figure 2b) with a compressible fluid. If the reservoir of pressurized fluid is large, the volume change due to the extension of the unbonded area (Figure 2c) will not significantly influence the pressure. To evaluate the first two terms in Equation 1, it is convenient to use Clapeyron's theorem, which states that for a linearly elastic body (7, p. 86)

> The strain energy of deformation is equal to one half of the work that would be done by the external forces (of the equilibrium state) acting through the displacements from the unstressed state to the state of equilibrium.

This theorem means that the second term in Equation 1 is always twice the magnitude of the first term and, for the constant-pressure system the rate of change of the second term due to crack extension is twice the rate of change of the first. Therefore, if the magnitude of either term can be calculated, the theorem can be used to evaluate the other.

For example, Timoshenko (8) gives the vertical displacements (w) of a circular plate with a fixed outer boundary and uniformly loaded with a pressure (p) to be

$$w(r) = (p/64D)(a^2 - r^2)^2 \qquad (3)$$

where

r = radial coordinate,
a = outside radius of plate, and
D = plate stiffness, i.e.,

$$D = Eh^3/12(1 - \nu^2) \qquad (4)$$

where

E = tensile modulus of elasticity,
ν = Poisson's ratio, and
h = plate thickness.

Equation 3 provides the uniform surface traction (p) and the displacements [w(r)] necessary to evaluate the second term of Equation 1, which becomes

$$\int_S T_i u_i ds = \int_o^a pw(r)2\pi r dr = (\pi p^2/32D)\int_o^a (a^2 - r^2)^2 r dr$$
$$= \pi p^2 a^6/192D \quad (5)$$

Clapeyron's theorem defines the first term as one-half this value, i.e.,

$$\int_V U dv = \pi p^2 a^6/384D \quad (6)$$

The third term, $\int_S \gamma_a ds$, where the subscript a denotes a fracture along a surface of adhesion, is a subject of some contention. When a cohesive fracture occurs, there is little debate; two free surfaces are created, one on each side of the crack tip as it advances through the material. The corresponding concept is not as obvious for an adhesive failure along a bond surface between dissimilar materials. Intuitively, it seems that such a schism might result in one new surface, two new surfaces, or possibly a fractional value between. Following the lead of others to accommodate each of these possibilities, we shall add a coefficient (c) to the third integral with the understanding that it can assume values in the range of $1 \le c \le 2$. In all subsequent calculations, c is assigned a value of 2.

The third integral can now be written as

$$\int_S \gamma_a ds = \int \gamma_a c 2\pi r dr = \gamma_a c 2\pi \int r dr = \gamma_a c \pi a^2 \quad (7)$$

The expression for PE now becomes

$$PE = (\pi p^2 a^6/384D) - (\pi p^2 a^6/192D) + \gamma_a c \pi a^2 \quad (8)$$

and to ensure that the variation with respect to the unbonded area is zero (i.e., that $\delta PE = 0$), $\partial PE/\partial a$ must be zero. Thus,

$$\partial PE/\partial a = (6\pi p_{cr}^2 a^5/384D) - (6\pi p_{cr}^2 a^5/192D) + 2\gamma_a c \pi a = 0 \quad (9)$$

is the energy balance equation defining the critical pressure (p_{cr}) necessary to cause the radius of the blister to begin to grow. If the pressure is insensitive to crack growth, there will be a catastrophic failure and the rapid removal of the entire plastic layer. The criticality equation can be rearranged to

$$\gamma_a = (3/32)/[(1 - \nu^2)/c](a/h)^3(p_{cr}^2 a/E) \quad (10)$$

and used to reduce the experimental test results to give γ_a.

Both the p and the w of the blister should be recorded. These data are then used to determine the effective modulus (E) for evaluating Equation 10. Equation 3, with r = 0, can be rearranged to give

$$E = (3/16)(1 - \nu^2)(a/h)^3 a(P/w) \quad (11)$$

which shows that E is directly proportional to the slope of the recorded p-versus-w curve.

When the blister is inflated with an incompressible fluid, the work done by the surface tractions during the growth of the unbonded area becomes zero. The stored strain energy decreases during growth, rather than increasing as with a compressible fluid. For this situation, the energy balance equation is written as

$$-(6\pi p_{cr}^2 a^5/384D) + 2\gamma_a c \pi a = 0 \quad (12)$$

and the critical pressure has the same value, regardless of the bulk stiffness of the pressurizing fluid (i.e., γ_a is given by Equation 10).

However, once crack growth begins, the subsequent behavior is different for the two types of pressurizing fluids. When a compressible fluid is used (i.e., pressure-controlled conditions), the unbonded area continues to grow without limit, but when an incompressible fluid is used (i.e., volume-controlled conditions), the unbonded area grows only slightly before the pressure decreases to below the critical value. From an experimental standpoint, this means that if an incompressible fluid is used as the loading medium, an incremental growth of

Figure 3. Theoretical solutions for thin and thick plates.

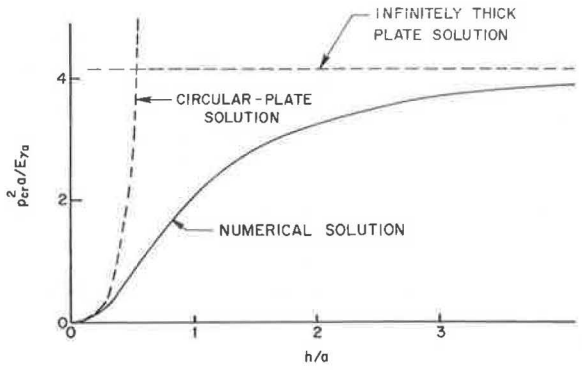

Figure 4. Solutions for small h/a ratios.

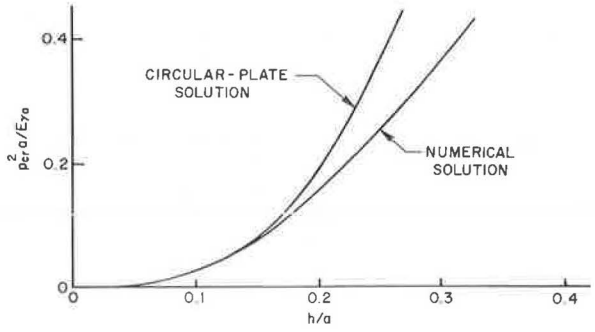

Figure 5. Wood form for casting concrete substrate.

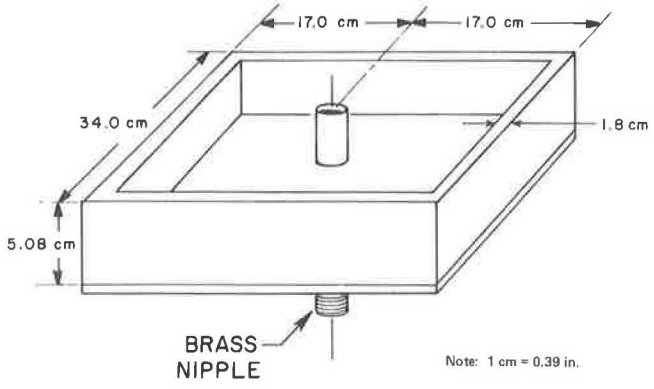

the unbonded area causes a loss of pressure due to the volume increase, and when the pressure drops below the critical value, growth is arrested. Immediately, however, the pressure increases, until it reaches a new critical value, at which time it decreases again, and the cycle is repeated. Thus, numerous data points can be obtained from only one sample. On completion of the test, the dimensions of the initially unbonded area for each cycle can be determined from the striations left on the concrete block.

The closed-form solutions, which are derived from the equations for the deflections of a flat circular plate, lose their validity as the ratio of the thickness to the radius increases. An analytical solution for the limiting case of a very thick plate (i.e., $h/a \to \infty$) has been derived by Mossakovskii and Rybka (9) to be

$$p_{cr} = \left(-[2\pi\gamma_a E(1 - 2\nu)c]/a(1 + \nu)(3 - 4\nu) \times \left\{[(\pi^2/4)\ln^{-2}(3 - 4\nu)] + 1\right\}\ln(3 - 4\nu)\right)^{1/2} \quad (13)$$

or, when $\nu = 1/2$

$$p_{cr} = (2c\pi/3)^{1/2}(E\gamma_a/a)^{1/2} \quad (14)$$

Figure 6. Teflon disk on concrete slab.

Figure 7. Schematic of test apparatus.

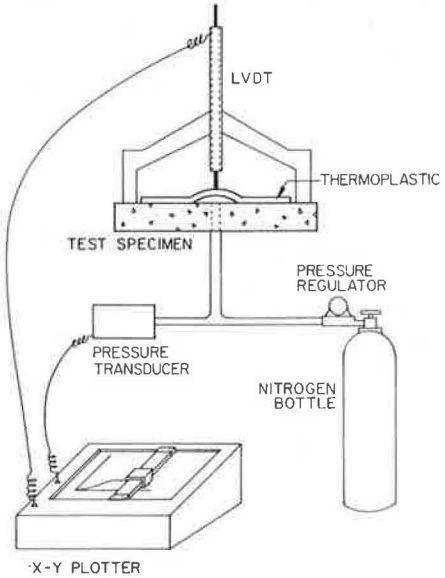

Equations 10 and 14 have been rewritten in a dimensionless format and are plotted, using dashed lines, in Figure 3. The abrupt intersection of these two closed-form solutions has been discussed in detail by both Williams (3) and Jones (4), who concluded that a practical transition curve between these two theoretical solutions is certain to exist.

Figure 8. Specimen before removal of failed thermoplastic.

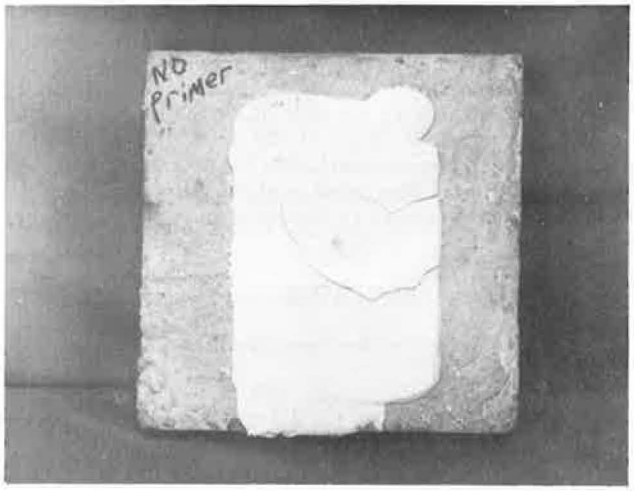

Figure 9. Specimen after removal of failed thermoplastic.

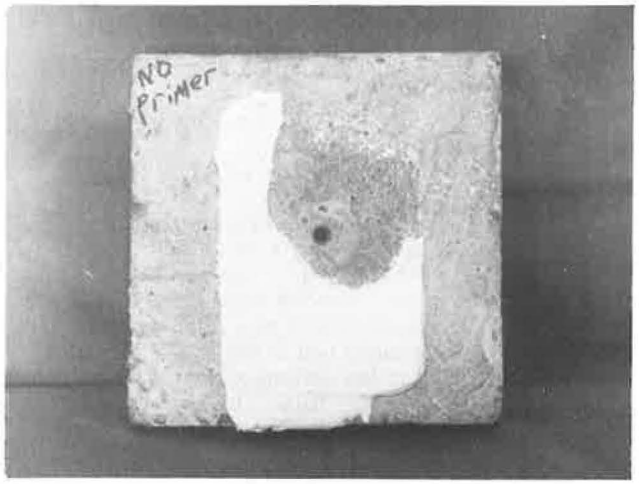

Figure 10. Previously bonded surface of thermoplastic.

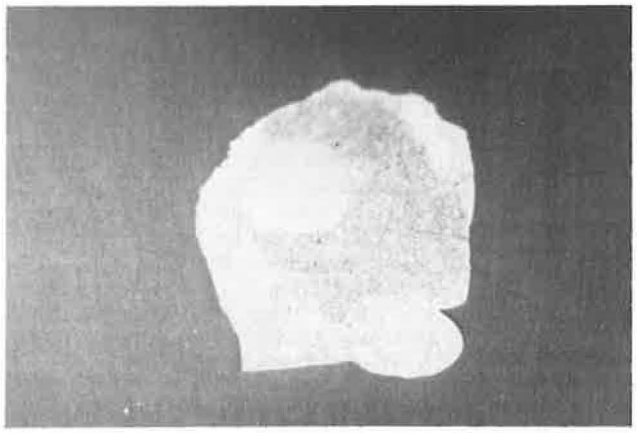

Bennett and others (6) have performed the numerical calculations necessary to define the transitional curve. By using finite elements, they calculated the rate of change of the stored strain energy with respect to the radius of the unbonded area with the pressure held constant, and by putting the numerical derivative equal to γ_a, are able to make the calculations for several h/a ratios and define the shape of the transition (the heavy line of Figure 3).

For the geometries used in the tests described, geometries that are typical of failures observed with actual thermoplastic highway markings, only a small portion of the numerical curve shown in Figure 3 is required. In all test specimens, the radius of the initially unbonded area was 2.22 cm (0.875 in); the thicknesses varied from 0.32 to 0.76 cm (0.125 to 0.3 in), so that the range of the ratio of the thickness to the radius was $0.15 < h/a < 0.35$. This portion of the curve in Figure 3 was enlarged as shown in Figure 4 and used to reduce the test data.

EXPERIMENTAL PROCEDURE

The experimental procedure required the following items of equipment:

1. A 30.5 by 30.5 by 5.1-cm (12 by 12 by 2-in) concrete panel with a 0.64 by 7.62-cm (0.25 by 3-in) (National) taper pipe thread brass nipple cast in the center,
2. A high-pressure bottle of nitrogen as a gas source and a regulator to provide pressures up to 414 kPa (60 lbf/in^2) (an inert gas was used so that the bond integrity would not be influenced),
3. A linear variable differential transducer (LVDT) with a range of at least 1.27 cm (0.5 in),
4. A pressure transducer with a range of 414 kPa,
5. An X-Y recorder,
6. A 5-V dc power source to drive the pressure transducer, and
7. A carrier amplifier for the LVDT.

The first step was to cast the concrete panels. The concrete was made of three parts small aggregate to two parts sand to one part type 1 portland cement, a typical paving mix. One of the threaded ends of the nipple was sawed off and mounted so that it was flush with the top of the form. The threaded end of the nipple extended through a hole bored in the bottom of the form, as shown in Figure 5. The form was filled with concrete until it was flush with the flat end of the nipple. The panels were cured 7 d at 22.8°C (73°F) and 95 percent humidity and allowed to dry at 60°C (140°F) for 7 d to ensure that the presence of water would not affect the test. In two instances, the top of the nipple was not exactly flush with the concrete surface, but this was remedied by carefully hand grinding the extrusion without affecting the surrounding concrete surface.

The panels were then brought back to 22.8°C at 25 percent humidity, and the thermoplastic material was applied. A 4.45-cm (1.75-in) diameter Teflon disk was centered over the nipple, as shown in Figure 6. In the experiments in which a primer was used, it was sprayed on to a thickness of approximately 50 μm (0.002 in). After all preparations were made, the thermoplastic material was centered over the Teflon disk and the air hole and applied at a temperature of 204°C (400°F). It was applied approximately 0.3 cm (0.13 in) thick by using a drawdown process in which the excess thermoplastic was removed with a spatula (laboratory simulation of an actual highway application). The panels and thermoplastic were cured at room temperature for a minimum of 24 h. The test was run in a 32°C (90°F) environment; therefore, the specimens were stored in this environment for another 24 h before testing to stabilize any temperature differentials.

Before the tests were run, the electronic signals being fed to the X-Y recorder were calibrated to a meaningful scale on the graph paper. The LVDT was mounted in a calibration block in which prescribed displacements could be imposed by turning a micrometer barrel. A distance of 2.54 cm (1 in) on the graph was found to correspond to a 0.13-cm (0.05-in) displacement of the LVDT. The pressure transducer signal was calibrated by plugging the open end of the tubing and increasing the pressure in increments of 69 kPa (10 lbf/in^2). Tick marks were made on the X-Y plotter at each increment: 3.05 cm (1.2 in) on the graph were equal to 69 kPa. These scales were used in interpreting the final plots.

In preparing the sample for testing, the LVDT was centered over the initially unbonded area and oriented to measure the vertical displacement of the thermoplastic. The LVDT signal was run through the carrier amplifier and fed to the Y-axis of the recorder. The pressure transducer and tubing from the gas bottle were threaded onto the nipple in a tee connection with the transducer placed as closely as possible to the panel connection to ensure the pressure recorded was essentially that experienced under the blister. The pressure signal was fed to the X-axis of the recorder. The system (Figure 7) was checked for leaks to ensure the accuracy of the plotted data.

After the connections were made, the X-Y recorder was zeroed. The pressure was increased manually at a constant rate of approximately 69 kPa/min at the regulator until leakage or failure occurred. Figures 8, 9, and 10 follow a sample to failure; Figure 8 shows the specimen before the thermoplastic is removed, Figure 9 shows it after the thermoplastic has been removed, and Figure 10 shows the lower surface of the failed thermoplastic. An interesting observation common to all samples is that the lower surface of the thermoplastic is honey combed (Figure 10), even though the exposed side has a glossy finish. The exact thickness of the specimen, a dimension needed for the calculations, was measured with a micrometer.

EXPERIMENTAL RESULTS

Six blister tests were made with the elementary apparatus described above. The resulting curves are shown in Figure 11 in which 11a and 11b show the results for the specimens without and with an adhesive respectively.

To calculate a meaningful value of γ_a between the concrete and the thermoplastic marking material, it is necessary to know the mechanical properties of the two materials. The concrete was assumed to be perfectly rigid so that equations derived above would be applicable. The effective tensile modulus of the thermoplastic was estimated by substituting the deflection of an elastic circular plate subjected to a uniform load normal to its surface into Equation 11. Because the value of the bulk modulus of the thermoplastic is many times greater than that of the tensile modulus, a value >0.49 at 32°C (90°F) was used for Poisson's ratio. Once a and h are known, the effective tensile modulus is seen to be linearly proportional to the slope of the p-versus-w curve. Figure 11 shows that these curves have decreasing slopes all the way to failure. Thus, the question then arises as to what slope should be used to calculate the modulus and, in turn, the adhesive energy release rate. Because an increase in the unbonded area, with the pressure held constant, will increase the stored strain energy, the modulus corresponding to the slope of the p-versus-w curve just before failure was chosen.

Figure 11. Measured pressure versus blister displacement: (a) without primer and (b) with primer.

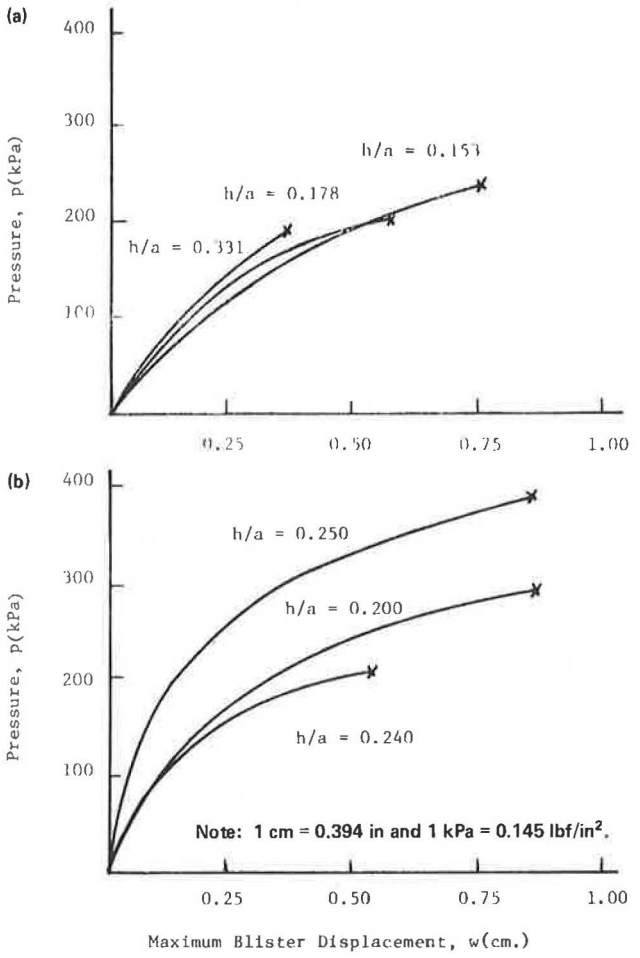

Table 1. Results of blister-peel tests of thermoplastic striping material on portland cement concrete.

Test	h (cm)	Tangent Modulus at Failure (kPa)	Geometric Coefficient	Characteristic Strain-Energy Release Rate (J/m²)
No adhesive				
1	0.340	17 200	0.082	998
2	0.396	8 300	0.120	990
3	0.737	1 900	0.440	1090
With adhesive				
4	0.498	2 800	0.202	2060
5	0.556	3 700	0.254	3960
6	0.445	5 400	0.156	2286

Note: 1 cm = 0.39 in, 1 kPa = 0.145 lbf/in², and 1 J/m² = 0.005 32 in·lbf/in².

When E and the pertinent dimensions are known, γ_a is readily calculated. The numerically derived curve of Figure 3 was entered with the appropriate value of h/a to find the geometric coefficient equal to $p_{cr}^2 a/E\gamma_a$. The γ_a values determined in this manner are shown in Table 1.

CONCLUSIONS

A sensitive test for the adhesion of thermoplastic highway-marking materials to pavements has been successfully demonstrated. The test gives quantitative values for the characteristic strain energy required to force crack growth along the bonded surface. The magnitude of this quantity (γ_a) reflects the ability of a bonded surface to resist the tendency to debond because of either external loadings, such as tires, snow studs, and snow plows, or to internally generated gas pressures.

As shown in Equations 12 and 14, the experimental evaluation of γ_a is a function of the square of the applied pressure at failure; i.e., the parameter is especially sensitive to random experimental errors of the measured value for p_{cr}. However, the results were quite reproducible, particularly when the rudimentary test apparatus used for the demonstration is considered.

The average value of γ_a at 32°C for the thermoplastic applied without an adhesive is 1025 J/m² (5.86 in·lb/in²) and that for the thermoplastic applied with an epoxy adhesive is 2869 J/m² (16.3 in·lb/in²).

Comparison of the results of earlier poker chip tests of the same thermoplastic and pavement combinations with and without the epoxy adhesive is interesting. In those tests, a small poker chip of thermoplastic, 5.1 cm (2 in) diameter by 0.5 cm (0.2 in) thick, was bonded to the pavement, and an aluminum platen, also 5.1 cm in diameter, was then bonded to the top of the thermoplastic. The platen was pulled away from the pavement and the force required to separate the thermoplastic from the pavement measured. At 23°C (73°F), the average bond strengths were 924 and 1530 kPa (134 and 222 lbf/in²) for the poker chip specimens with and without adhesive respectively.

The significance of these tests is unclear, however, because of the complex state of stress generated within the thermoplastic and because the failures often do not originate or propagate along the bonded (thermoplastic to pavement) surface.

The advantages of using γ_a to compare various highway-marking systems are obvious. The test can be performed with a minimum of equipment by relatively inexperienced technicians under a variety of environmental conditions. Either a liquid or a gas can be used for the pressurization, which means that the deleterious effects of entrapped extrinsic chemicals can be evaluated. That γ_a can actually be used to calculate the margin of safety for the bonded surface under specified loads is not without its advantages.

Many unanswered questions remain. Probably the most important is the determination of how γ_a changes as a function of temperature and rate of loading. Another is the determination of how it changes during the curing period just after the thermoplastic is placed. But eventually, the test should provide a sensitive method for evaluating the bond performance of a given thermoplastic highway-marking system. The influence of variables that can be anticipated, reproduced in the laboratory, and defined in numerical terms useful to the engineer is particularly important.

REFERENCES

1. Thermoplastic Pavement Markings. Iowa Department of Transportation, Final Rept., 1975.
2. H. Dannenberg. Measurement of Adhesion by a Blister Method. Journal of Applied Polymer Science, Vol. 5, No. 14, 1961, pp. 125-134.
3. M. L. Williams. The Continuum Interpretation for Fracture and Adhesion. Journal of Applied Polymer Science, Vol. 13, No. 1, 1969, pp. 29-40.
4. W. B. Jones. A Simple Test for Certain Cases of Adhesion. College of Engineering, Univ. of Utah, Rept. UTEC DO-69-010, 1969.
5. J. D. Burton, W. B. Jones, and M. L. Williams. Theoretical and Experimental Treatment of Fracture in an Adhesive Interlayer. Trans., Society of Rheology, Vol. 15, No. 1, 1971, pp. 39-50.

6. S. J. Bennett, K. L. DeVries, and M. L. Williams. Adhesive Fracture Mechanics. International Journal of Fracture Mechanics, Vol. 10, No. 1, 1974, pp. 33-43.
7. I. S. Sokolnikoff. Mathematical Theory of Elasticity. McGraw-Hill, New York, 1956.
8. S. Timoshenko and S. Woinowsky-Krieger. Theory of Plates and Shells. McGraw-Hill, New York, 1959.
9. V. I. Mossakovskii and M. T. Rybka. Generalization of the Griffith-Sneddon Criterion for the Case of a Non-Homogeneous Body. Prikladnaya Matematika I Mekhanika, Vol. 28, 1964, pp. 1061-1069.

Publication of this paper sponsored by Committee on Coatings, Signing, and Marking Materials.

Vehicle Corrosion in Perspective

Michael C. Belangie, Materials and Research Section, Utah Department of Transportation

Early perforation corrosion of American manufactured vehicles was a limited localized phenomenon before the mid-1950s, but a short time after the introduction of unibody construction and sculptured styling in 1955, its occurrence became common throughout most of the United States. The use of deicing salts, which had approximately doubled between 1953 and 1956, was cited in some of the literature of the period as the probable cause. There was little mention of the reduction in sheet-metal thickness that accompanied the change to unibody construction. Anticorrosion measures were nominal in the period immediately following the adoption of unibody construction. The period before the mid-1960s was not typified by major advances in anticorrosion technology, but was a period of trial and error with much of the emphasis being placed on improved anticorrosion design practice. It is doubtful that the improvements made in this period (1958 to 1965) could have counteracted the effect of the sevenfold increase in deicing salt use during 1953 to 1965 if deicing salts were the principal cause. Although it appears that the changes in manufacturing practice were the principle cause of widespread corrosion, the modifications in that practice since the change are producing significantly more corrosion-resistant vehicles. Low-priced, 1955 and 1956 vintage automobiles having unibody construction began to perforate within 6 months in severely corrosive environments. In late 1976, one motor company of Canada began warranting its cars for 36 months against perforation.

It is pertinent to the following discussion to remember the prejudicial character of the deicing salt versus corrosion controversy and that fixed in the minds of many persons in this country is the conviction that deicing salt is the principal cause of automobiles rusting.

The questions addressed here are these. First, Is the opinion that deicing salts are the principal cause of vehicle corrosion damage legitimate? And second, If it is not legitimate, how much of the depreciation in the value of the average automobile can be assessed to deicing salts? These questions are not casual. In January, 1975, the research section of the Utah Department of Transportation became the lead agency in an 11-state pooled-fund study that included Idaho, Illinois, Maryland, Michigan, Minnesota, Montana, New Hampshire, South Dakota, Utah, Virginia, and Washington and the Federal Highway Administration. The purpose of this study was to develop an economic model for snow and ice control activities (1). However, the funding was insufficient to allow the type of economic analysis of vehicle corrosion that would be necessary to effectively determine the portion of increased automotive depreciation costs that can be attributed to deicing salt. As an alternative, an in-depth review of the literature was made. More than 200 publications on vehicle corrosion were collected: Of this number, more than 80 percent were technical, as opposed to economic or summation, documents. Of the technical documents, many came from the Society of Automotive Engineers and the National Association of Corrosion Engineers. The essence of this collection is summarized in an unpublished draft, Vehicle Corrosion, a Synthesis (2).

In developing this synthesis, it became apparent that the document collection could be divided into two sections: those documents or portions of documents dealing with the corrosivity of the environment and those dealing with the ability of the vehicle to resist corrosion. The differentiation is important in evaluating and assigning relative economic costs because it accentuates the fact that both the ability of the average vehicle to resist corrosion and the corrosivity of the environment have varied over time. This makes the assessment of costs due to corrosion considerably more complex than would be indicated by recent economic studies.

An understanding of the market place may be adequate to determine the additional depreciation of the average automobile of a given vintage due to corrosion. However, it is not sufficient to determine the assessment of costs against one environmental factor. To make this assessment, a basic understanding of the variability of the corrosive environment as well as of the changing technology of the average automobile is mandatory.

CORROSIVE ENVIRONMENT

What factors then must be considered if one wishes to assess the cost of a specific corrosion-causing environmental factor, in this case, deicing salts? The size and extent of the corrosive environment is probably a reasonable starting point.

Figure 1 indicates that vehicle corrosion is a worldwide phenomenon. The map shows the noncommunist areas having the potential for a substantial degree of corrosion. Blackened areas indicate the probable use of deicing salts; slashed portions show those areas that do not use salt. Unshaded areas are not exempt from corrosion, but in these areas, it is likely to occur so late in the economic lifetime of the average vehicle as to have relatively little effect on its resale value.

Of the 282 million vehicles registered in noncommunist countries in 1973 (3), approximately 55 percent were in corrosive environments in which deicing salts were apt to be used (blackened areas). Twenty-five percent were in equally corrosive environments in which no deicing salts were used (slashed areas). And 20 percent were in environments where corrosion occurs, but is generally not considered a substantial problem.

Of the 102 million automobiles registered in the United States in 1973 (3), between 46 million and 74